The 2018 Structures Congress (Structures18)
Songdo Convensia, Incheon, Korea, August 27 - 31, 2018

Application of a negative stiffness device in the benchmark problem for a highway bridge

* Tong Sun [1)], Zhilu Lai [2)], Yichao Zhang[3)], Hongnan Li [4)] and Satish Nagarajaiah [5)],

[1), 3), 4)] *Department of Civil Engineering, Shenyang Jianzhu University, Shenyang, China*
[2), 5)] *Dept. of Civil and Environment Engineering, Rice University, Houston, America*
[1)] *tsun@sjzu.edu.cn*

ABSTRACT

In this study, the effectiveness of a novel NSD and damper system for reduction of seismic response of a highway bridge is investigated. To this end, a Phase II benchmark highway bridge is employed for its numerical evaluation. By engaging the NSD at an appropriate “apparent yield” displacement, the combination of isolation system and the NSD device behaves like a softening system. Excess deformation caused by stiffness weakening can be reduced by adding passive damping in parallel. Numerical simulation shows that the proposed passive NSD and damper system is beneficial in reducing seismic response of base isolated bridges.

KEYWORDS: base isolation; benchmark problem; negative stiffness device; seismic response control.

INTRODUCTION

Highway bridges are lifeline structures and hence their damage during earthquakes can have severe consequences. As a result, different types of protection devices (passive, active and semi-active) have been analyzed, tested and implemented. Conventional passive methods of strengthening rigid connection between deck and substructure is effective in reducing deck displacement, but at the expense of increasing the pier base shear. Furthermore, in near-fault ground motion conditions, strong velocity pulses can amplify the dynamic response of the isolated bridge when the pulse period is close to the fundamental period (Shen 2004).

In addition to passive devices, many active and semi-active systems have been

---

[1)] Assistant Professor
[2)] Graduate Student
[3)] Assistant Professor
[4)] Professor
[5)] Professor

developed and implemented in bridges to modify the damping and stiffness of the structure. Spencer et al. (Spencer 1997) demonstrated that MR fluid dampers can generate large damping force without high power requirement. Sahasrabudhe and Nagarajaiah (Sahasrabudhe 2005) conducted experimental and numerical studies on semi-active control of sliding isolated bridges using magneto-rheological (MR) dampers and variable stiffness systems. Iemura and Pradono (Iemura 2003) showed an application of pseudo-negative stiffness control in benchmark cable-stayed bridge; numerical simulations show that the control system is beneficial in reducing both the base shear and the deck displacement. Tan et al. (Tan 2009) presented sample passive, semi-active and active control system designs for the seismically excited benchmark highway bridge. Previous investigations have demonstrated the effectiveness of semi-active devices in reducing the earthquake response of the structure. However, compared to passive devices, the requirement of external power and feedback signal reduce the reliability of semi-active and active control systems.

To reduce both acceleration and base shear, Reinhorn et al.(Reinhorn 2005) introduced the concept of weakening of structures which is effective but will lead to reduction of strength, and cause permanent damage. Pasala et al.(Pasala 2012) developed and tested a new adaptive negative stiffness device that could create true negative stiffness behavior to reduce earthquake responses through ‘apparent weakening’ (not actual weakening structure strength). By activating the NSD at certain displacement, the combined behavior of the whole system has a much earlier yield point, than the primary structure, which enables significant base shear and displacement response reductions when used in parallel with a fluid damper. In addition, Attary et al. (Attary 2015) demonstrated the effectiveness of the adaptive negative stiffness system for seismic protection of base isolated bridges. The NSD presented in this study is completely new and different from the earlier version (Pasala 2012) and is quite novel and scalable.

To compare the performance and effectiveness of various control systems, a benchmark problem on highway bridges has been developed by Agrawal et al.(Agrawal 2009). Phase I problem studies the case when the bridge deck is fixed to the outriggers (or piers appropriately). In phase II, the bridge deck is isolated from the outriggers by lead-rubber bearings as shown in Figure 1. The present study is based on phase II.

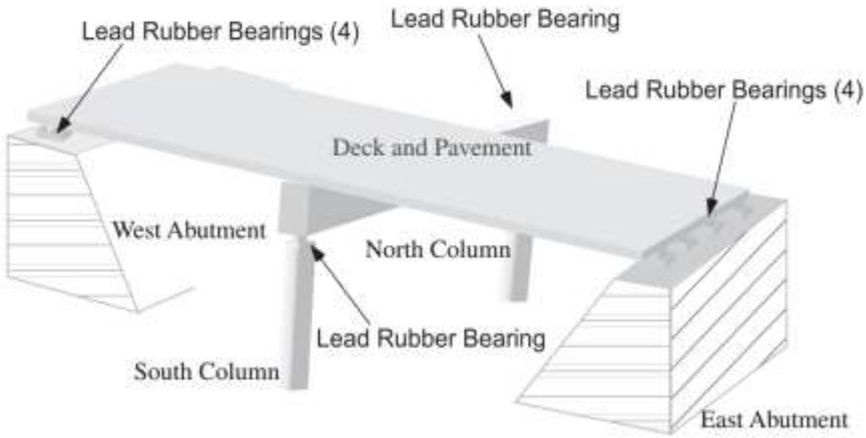

Figure 1. Schematic of the highway bridge benchmark [8]

The present paper investigates the performance of a novel negative stiffness device for the earthquake protection of the benchmark highway bridge through numerical simulations. Passive dampers are employed to control the excessive displacement caused by lower horizontal effective stiffness due to the introduction of NSD. Results from shaking table tests of the NSD are presented to verify the analytical model of the device. The effectiveness of the NSD system in reducing the response of bridge benchmark problem is evaluated numerically.

THE BENCHMARK HIGHWAY BRIDGE

The bridge model used for benchmark study is based on the 91/5 highway bridge in Southern California. The superstructure of the bridge consists of two-span, cast-in-place pre-stressed concrete (PC) box-girder and substructure is in the form of PC outriggers. Each span of the bridge is 58.5m long, spanning a four-lane highway, with two abutments are skewed at 33° . The width of the deck is 12.95m along the east and 15 m along the west direction. The deck is supported by a 31.4m long and 6.9m high pre-stressed concrete outrigger, resting on two pile groups. The total mass of the benchmark highway bridge is 4,237,544kg and the mass of the deck is 3,278,404kg.
In order to compute the structure properties, a full 3-D finite-element model with 430 degrees of freedom has been developed in ABAQUS by Agrawal et al. (Agrawal 2015). The superstructure is modeled by B31 element and rigid links are used to connect the control devices. In phase II, a total of 20 control devices (10 in each direction) are placed at the ten lead rubber isolation bearing locations as shown in Figure 2.

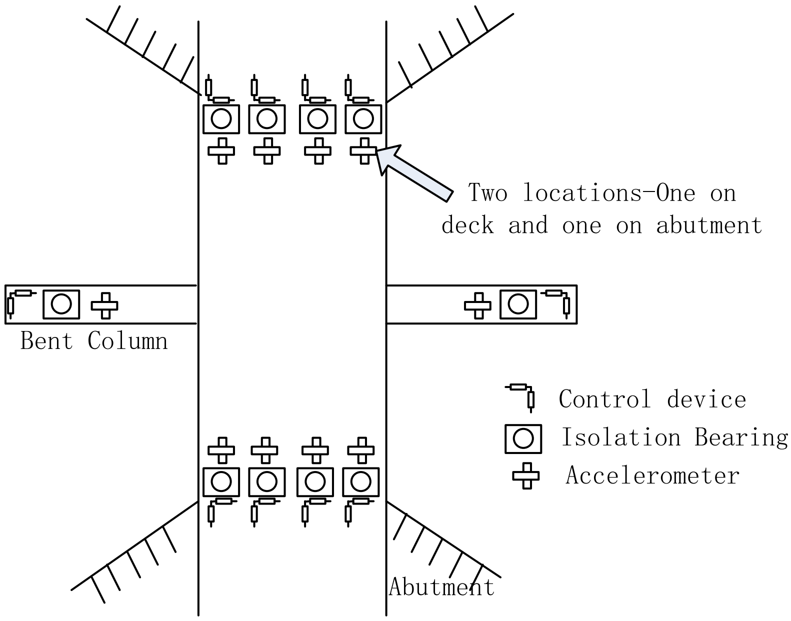

Figure 2. Locations of control devices and sensors on the bridge [8]

A set of 21 evaluation criteria has been developed to evaluate the effectiveness of different control schemes. Readers are referred to the definition paper (Agrawal 2015) for more details.

DESCRIPTION OF NEGATIVE STIFFNESS DEVICE

As shown in Figure 4, the negative stiffness device developed in this work consists of a roller pushed by a pre-compressed spring and a block with predesigned curve that the wheel can roll on. There is a flat gap on the curve around equilibrium, so that the stiffness of the combination of NSD and isolation system will be the same as that of the original isolation system only. When the roller goes beyond the gap, the pre-compressed spring (1) and the slope (3) will generate a force *F* in the same direction as the imposed displacement, thus the composite system appears to yield or soften i.e., apparent yielding. The negative force *F* is given by

$$F = F_n + F_f \tag{1}$$

Where, F_n is the force in x direction with displacement also occurring in the same direction (thus producing negative stiffness); F_f is component of the friction force. These forces are given by Eq. (2) and Eq. (3):

$$F_n = N \cdot \sin\alpha \cdot \cos\alpha = N \cdot \frac{\tan\alpha}{1+\tan^2\alpha} \tag{2}$$

$$F_f = -\operatorname{sgn}(\dot{x})\mu N \cos^2\alpha = -\operatorname{sgn}(\dot{x})\mu N \frac{1}{1+\tan^2\alpha} \tag{3}$$

Where *N* is the pre-compression force in the spring, α is the angle between tangent line at contact point and x axis. μ is the friction coefficient between the roller and the curve block.

Figure.3. Negative stiffness device with predesigned curve

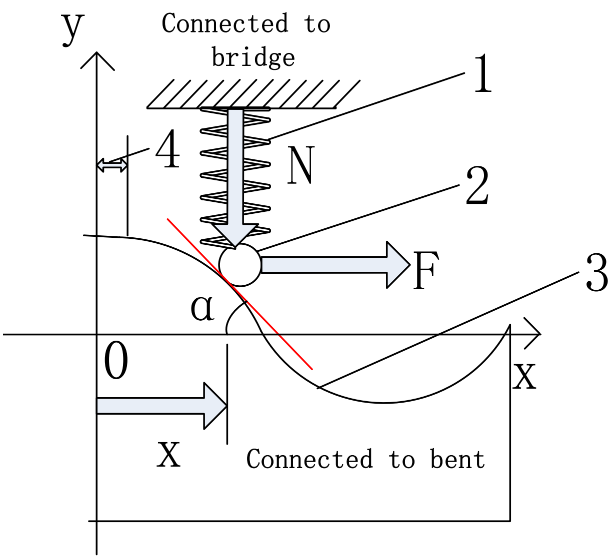

Figure. 4. Basic mechanism of the NSD
[1. Pre-compressed spring, 2. roller, 3. curve block, 4. flat gap]

Assume curve function is $y = f(x)$, where the amplitude of $f(x)$ is *A*, spring is pre-compressed by ΔL, *k* represent stiffness of the pre-load spring. *N* is given by

$$N = k \cdot \left[\Delta L - \frac{A}{2} + f(x) \right] \tag{4}$$

Substituting Eq.s (2), (3) and (4) into Eq. (1), the force generated by the NSD is expressed as:

$$F = k\left[\Delta L - \frac{A}{2} + f(x) \right] \cdot \frac{f'(x)}{1 + (f'(x))^2} - \mathrm{sgn}(\dot{x})\mu N \cos^2 \alpha \tag{5}$$

This Eq. indicates that the amount of the negative stiffness is controlled by the stiffness of pre-load spring, pre-compression, and the shape of the predesigned curve.

EXPERIMENTAL TESTING OF THE PROPOSED NEGATIVE STIFFNESS DEVICE

Experimental tests were carried out in order to determine the force characteristics of the NSD and provide validation to the proposed analytical model. Figure 6 shows the single degree of freedom (SDOF) experimental test setup.

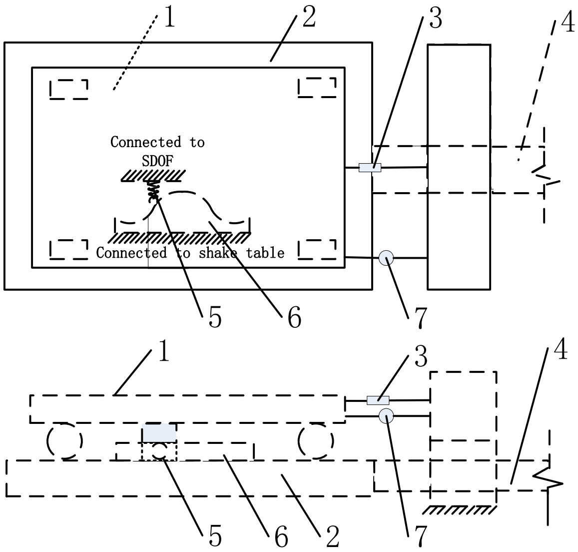

Figure 5. Schematic Diagram of the Experiment Setup [1.*SDOF*, 2.shake table, 3.load cell, 4. actuator, 5.precompressed spring , 6.curve block, 7.LVDT]

Figure 6. Experimental setup

A SDOF oscillator was assembled on the shake table, negative stiffness device was installed between the oscillator and the shaking table. As shown in Figure 5, the curve block is connected to shake table and the spring is fixed to the SDOF oscillator. The actuator was commanded to produce sinusoidal displacement that is applied to the shaking table. The SDOF was constrained from movement by a rigid rod with a load cell attached to the bulkhead near the actuator, so that the device is subjected to cyclic displacements. Excitation frequency was 0.1Hz, with amplitude of 5.08mm (0.2 inch).The predesigned function of the curve is

$$
\begin{aligned}
&\text{If} \quad x \le -6.35 && y = 6.35 \cdot \cos\left[\frac{2\pi}{3} \cdot (x + 6.35)\right] \\
&\text{If} \quad -6.35 \le x \le 6.35 && y = 6.35 \\
&\text{If} \quad 6.35 \le x && y = 6.35 \cdot \cos\left[\frac{2\pi}{3} \cdot (x - 6.35)\right]
\end{aligned}
\tag{6}
$$

In which the length unit is millimeter (mm). The stiffness of the preload spring is 19.3 N/mm (110 pound/inch). The pre-compression is 12.70 mm (0.50 inch). A comparison of experimental test result with the analytical model is shown in Figure 7. As seen from the figure, the theoretical results agree well with the experimental result. It can be concluded that the analytical model is sufficient for adequately capturing the NSD behavior.

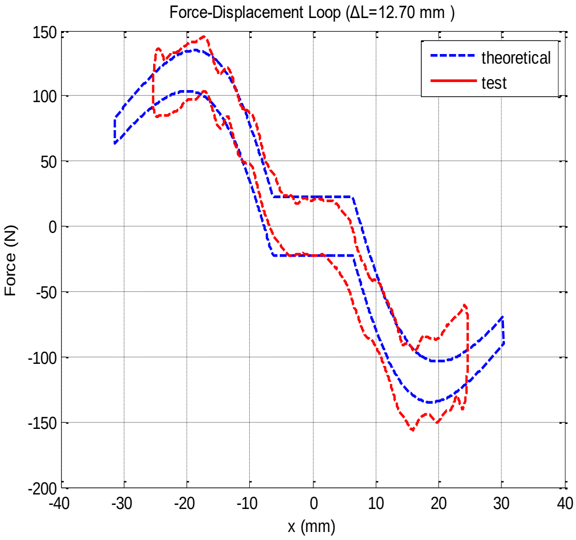

Figure 7. Verification of the analytical model

APPLICATION TO BENCHMARK HIGHWAY BRIDGE MODEL

Based on the NSD model parameters obtained from the shaking table test, the parameters of the NSD are obtained (by running as series of simulations that resulted in the least response) for application to the bridge benchmark model. The optimal parameters are given in Table 1.

Table 1. Values of NSD parameters obtained for application to the bridge benchmark model

Parameter	Value	
Stiffness of pre-compressed spring	410 kN/m	
ΔL	1.5 m	
Curve function	If $x < -0.13$	$y = 0.5 \cdot \cos[1.5 \cdot (x + 0.13)]$
(m)	If $-0.13 \leq x \leq 0.13$	$y = 0.5$
	If $0.13 < x$	$y = 05 \cdot \cos[1.5 \cdot (x - 0.13)]$

A passive damper is employed in the system to limit the excessive displacement caused by introduction of the NSD. The properties of the passive damper are optimized by the method proposed by Cimellaro et al. (Cimellaro 2009). Damping ratio is set to be 20% of critical. Damping force developed by the damper is given by

$$F_{PD} = 2\xi\sqrt{K_e m}\dot{x} \qquad (7)$$

Where the F_{PD} is the damper force, ξ is the damping ratio, K_e and m represent the stiffness of the mass of the structure system, respectively. $\dot{x}$ is the velocity of the connection point relative to base (Pasala 2012).

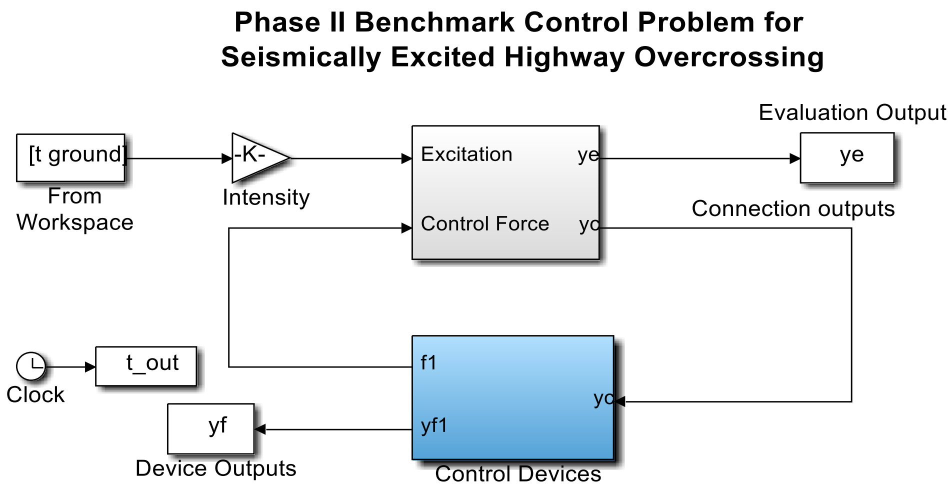

Figure 8. Modified block with NSD and passive dampers

The application of the proposed NSD to the Phase II base-isolated highway bridge model is achieved by modifying the SIMULINK block in the benchmark problem as shown in Figure 8. The number and location of the NSD are the same as those in sample controller for the fully base-isolated case (Nagarajaiah 2009).

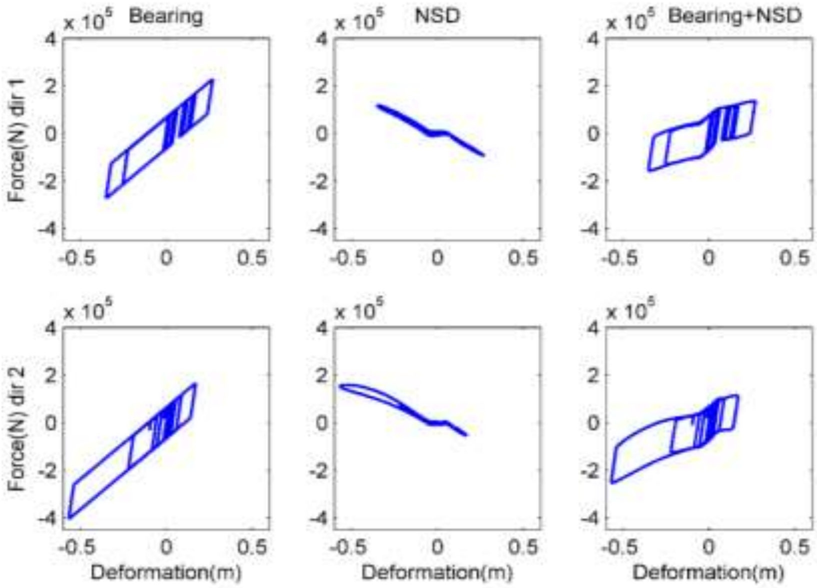

Figure 9. Damper and bearing hysteretic loops at node No. 101 (in directions 1 and 2) under Rinaldi Earthquake.

Figure 9 shows the hysteretic loops of the bearings, the NSDs, and combined hysteresis loops of bearing/NSD at the node NO. 101 in the direction 1 and 2. As can be seen in Figure 9, the NSD introduces an apparent yield point in the system, and reduces the stiffness past apparent yielding displacement of the system. In addition the damper in parallel produces larger damping ratio. Lower stiffness past apparent yield displacement results in the reduction of transmitted force, but increases bearing deformation which is limited by higher damping provided by the passive damper added in parallel with the NSD.

Evaluation criteria of the proposed approach for the highway benchmark bridge model are shown in Table 2. A total of six historical earthquake records are considered. For comparison purposes the results of sample semi-active （SS） and sample passive (SP) controller (Cimellaro 2009) are also presented. Figure 10 shows the graphical representation of the comparison of the base shear, displacement and acceleration evaluation criteria for three cases. It is observed from Figure 10 that the base shear is generally lower with the proposed NSD and damping (ND) system. The proposed approach can reduce the peak base shear by more than 20% compared to sample semi-active and sample passive control, respectively. It is clear that the proposed NSD and damper system reduces shear, while keeping the bearing deformation within bounds. Decrease in base shear is mainly due to the 'apparent yielding' or reduction in stiffness past the apparent yield displacement (as evident in the force deformation loops of the bearing/NSD in the figures of last column of Figure 10). The stiffness reduction is due to the negative stiffness of the NSD device, which follows the initial zero stiffness due to gap (equal to the apparent yield displacement), as seen in the figures of middle column of Figure 10. The increased base displacement caused by the NSD is reduced by the addition of passive damper.

The NSD with fluid damper system produces the less base shear (J_1<1 indicating reductions), less mid-span displacement (J_3<1) and less bearing deformation (J_5<1) , as shown in Figure 10, when compared to the other two cases of sample passive and sample semiactive; except, for the Chi-Chi earthquake. However, higher accelerations occur in the case of Kobe earthquake for both NSD with fluid damper system and the sample semiactive system.

The important thing to take note is that the NSD and damper passive system is able to mimic response reduction in the semiactive case, with a slightly better reductions in base shear (J_1<1) and slightly less reductions in the mid-span displacement and bearing deformations (J_5<1), and with nearly the same performance in mid-span accelerations (J_4>1). It is very interesting to note that NSD and damper system—a completely passive system—can produce comparable response reductions as the semiactive case (which requires external power) in an average sense—i.e., NSD system is slightly better in two evaluation criteria related to base shear and acceleration and the semi-active system is slightly better in two evaluation criteria related to displacement or bearing deformation.

Table 2 Performance Evaluation

Evaluation criteria	Control strategy	Npalmspr	Chichi	Elcentro	Rinadi	TurkBolu	Kobe_NIS
J1:Pk. base shear	ND	0.98	0.80	0.67	0.98	0.66	0.71
	SS	0.92	0.92	0.76	0.90	0.83	0.89
	SP	1.06	0.91	0.62	1.07	0.78	0.91
J2:Pk. over.mom.	ND	1.21	0.83	0.66	0.95	0.70	0.79
	SS	1.03	0.89	0.71	0.86	0.87	0.85
	SP	1.10	0.95	0.61	1.04	0.70	0.90
J3:Pk. mid. disp.	ND	0.69	0.87	0.47	0.76	0.53	0.32
	SS	0.56	0.74	0.36	0.69	0.36	0.26
	SP	0.87	0.76	0.50	0.90	0.59	0.83
J4:Pk. mid. acc.	ND	1.55	1.10	1.29	1.08	1.00	1.75
	SS	1.57	1.13	1.35	1.34	1.15	1.91
	SP	1.17	1.13	1.09	1.05	0.92	1.16
J5:Pk. Bear. Def.	ND	0.71	0.86	0.50	0.77	0.50	0.31
	SS	0.56	0.74	0.35	0.70	0.38	0.27
	SP	0.88	0.76	0.49	0.90	0.56	0.83
J6:Pk. ductility	ND	1.21	0.83	0.67	0.95	0.70	0.79
	SS	1.03	0.89	0.71	0.86	0.87	0.85
	SP	1.10	0.95	0.61	1.04	0.70	0.90
J9: nor. Base shear	ND	1.14	0.67	0.87	0.78	0.33	0.51
	SS	0.67	1.01	0.54	0.74	0.43	0.53
	SP	1.19	0.98	0.66	0.84	0.58	0.97
J10: nor. over.mom.	ND	1.16	0.67	0.86	0.75	0.33	0.49
	SS	0.66	1.00	0.51	0.70	0.42	0.52
	SP	1.21	0.98	0.60	0.82	0.58	0.96
J11: nor. mid. disp.	ND	0.88	1.26	0.70	0.55	0.16	0.28
	SS	0.43	0.90	0.32	0.46	0.32	0.28
	SP	1.02	0.98	0.59	0.76	0.52	0.96
J12: nor. mid. acc.	ND	1.14	1.57	1.02	1.17	0.96	1.14
	SS	1.59	1.58	1.23	1.24	1.13	1.19
	SP	0.91	1.19	0.95	0.98	0.87	0.99
J13: nor. bear. def.	ND	0.89	1.53	0.74	0.56	0.16	0.29
	SS	0.42	0.91	0.33	0.46	0.34	0.28
	SP	1.03	0.98	0.62	0.76	0.52	0.96
J14: nor. ductility	ND	1.16	0.67	0.86	0.75	0.33	0.49
	SS	0.66	1.00	0.51	0.70	0.42	0.52
	SP	1.21	0.98	0.60	0.82	0.58	0.96
J16:Pk. stroke	ND	0.71	0.86	0.50	0.77	0.50	0.31
	SS	0.56	0.74	0.35	0.70	0.38	0.27
	SP	0.88	0.76	0.49	0.90	0.56	0.83

ND=NSD+Damper; SS=Sample Semi-active; SP=Sample Passive.

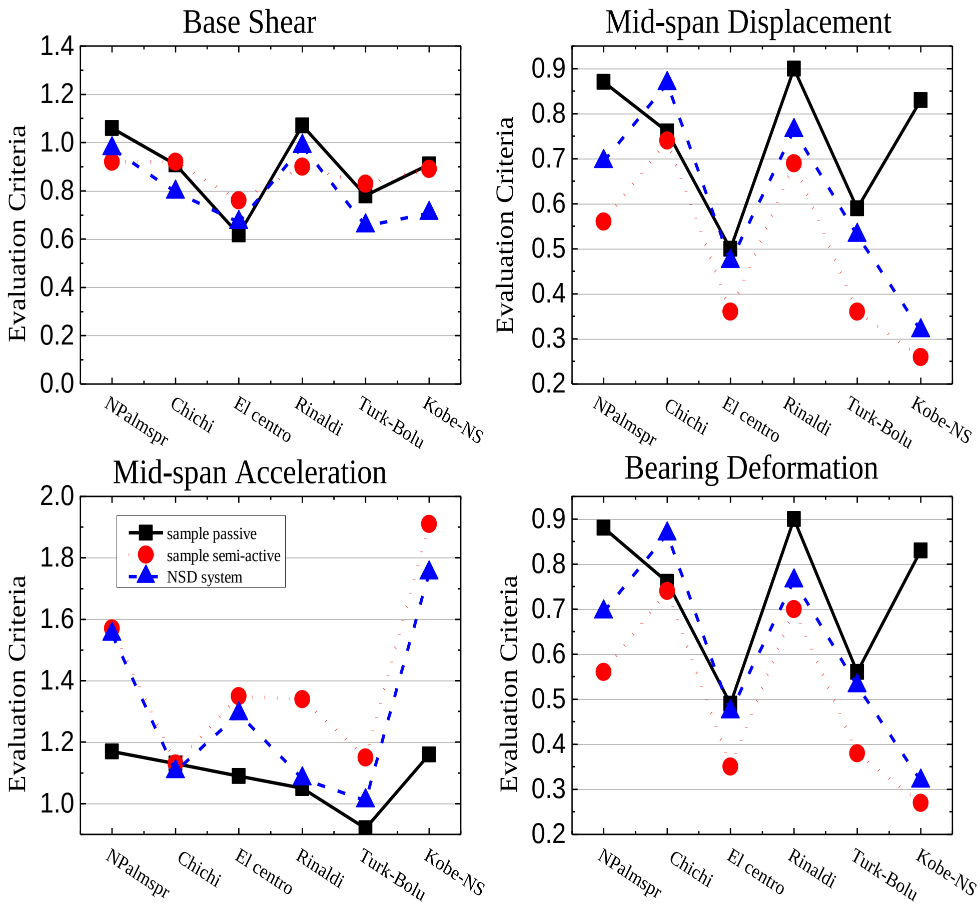

Figure 10. Graph of evaluation criteria for the sample passive control, sample semi-active control and proposed NSD and damper system.

CONCLUSION

This study investigates performance of a new NSD and damper system and its effectiveness in reducing the response in Phase II benchmark highway bridge problem. The proposed NSD passive system produces negative stiffness which enables apparent softening past a certain "yield" displacement. The combination of the NSD and damping force along with bearing force results in a behavior that reduces the base shear thus attracting it away from the main structure. The effectiveness of the proposed NSD and damper system is evaluated in comparison with the sample passive and semi-active controllers. The result shows that the proposed approach achieves lower base shear than those by the sample passive control and semi-active control. The NSD and damper system produces comparable reductions as that of the semi-active control but by completely passive means. The advantage of the proposed NSD is that the behavior of the device can be adjusted easily by changing the curve function and spring stiffness. The proposed passive approach has significant practical application potential because of the simplicity and the effectiveness of the device.

REFERENCES

Agrawal, A., Tan, P., Nagarajaiah, S., and Zhang, J. (2009). "Benchmark structural control problem for a seismically excited highway bridge—Part I: Phase I problem definition." *Structural Control and Health Monitoring*, 16(5), 509-529.

Attary N, Symans M, Nagarajaiah S, et al. (2015) “Experimental Shake Table Testing of an Adaptive Passive Negative Stiffness Device within a Highway Bridge Mode”, *Earthquake Spectra*, 31(4): 2163-2194.

Cimellaro, G. P., Soong, T., and Reinhorn, A. (2009). "Integrated design of controlled linear structural systems." *Journal of structural engineering*, 135(7), 853-862.

Iemura, H., and Pradono, M. H. (2003). "Application of pseudo‐negative stiffness control to the benchmark cable‐stayed bridge.", *Journal of Structural Control*, 10(3-4), 187-203.

Nagarajaiah, S., Narasimhan, S., Agrawal, A., and Tan, P. (2009). "Benchmark structural control problem for a seismically excited highway bridge—Part III: Phase II Sample controller for the fully base‐isolated case." *Structural Control and Health Monitoring*, 16(5), 549-563.

Pasala, D., Sarlis, A., Nagarajaiah, S., Reinhorn, A., Constantinou, M., and Taylor, D. (2012). "Adaptive negative stiffness: new structural modification approach for seismic protection." *Journal of Structural Engineering*, 139(7), 1112-1123.

Reinhorn, A. M., Viti, S., and Cimellaro, G. (2005) "Retrofit of structures: Strength reduction with damping enhancement." *Proc., Proceedings of the 37th UJNR panel meeting on wind and seismic effects*, Tsukuba.

Sahasrabudhe, S. S., and Nagarajaiah, S. (2005). "Semi-active control of sliding isolated bridges using MR dampers: an experimental and numerical study.", *Earthquake Engineering and Structural Dynamics*, 34(8), 965-984.

Shen, J., Tsai, M., Chang, K., and Lee, G. (2004). "Performance of a Seismically Isolated Bridge under Near-Fault Earthquake Ground Motions.", *Journal of Structural Engineering*, 130(6), 861-868.

Spencer Jr, B., Dyke, S., Sain, M., and Carlson, J. (1997). "Phenomenological model for magnetorheological dampers.", *Journal of engineering mechanics*.

Tan, P., and Agrawal, A. K. (2009). "Benchmark structural control problem for a seismically excited highway bridge—Part II: phase I sample control designs.", *Structural Control and Health Monitoring*, 16(5), 530-548.